Original

Feser, F.:

Enhanced detectability of added value in limited area model results separated into different spatial scales

In: Monthly Weather Review (2006) AMS

DOI: 10.1175/MWR3183.1

Enhanced Detectability of Added Value in Limited-Area Model Results Separated into Different Spatial Scales

FRAUKE FESER

Institute for Coastal Research, GKSS Research Centre, Geesthacht, Germany

(Manuscript received 15 July 2005, in final form 10 October 2005)

ABSTRACT

Regional climate models (RCMs) are a widely used tool to describe regional-scale climate variability and change. However, the added value provided by such models is not well explored so far, and claims have been made that RCMs have little utility. Here, it is demonstrated that RCMs are indeed returning significant added value. Employing appropriate spatial filters, the scale-dependent skill of a state-of-the-art RCM (with and without nudging of large scales) is examined by comparing its skill with that of the global reanalyses driving the RCM. This skill is measured by pattern correlation coefficients of the global reanalyses or the RCM simulation and, as a reference, of an operational regional weather analysis. For the spatially smooth variable air pressure the RCM improves this aspect of the simulation for the medium scales if the RCM is driven with large-scale constraints, but not for the large scales. For the regionally more structured quantity near-surface temperature the added value is more obvious. The simulation of medium-scale 2-m temperature anomaly fields amounts to an increase of the mean pattern correlation coefficient up to 30%.

1. Introduction

Regional climate models (RCMs) are a widely used tool to derive regionally specific information about the statistics of weather (i.e., climate), trends, and possible future changes. Such models feature an atmospheric limited-area model combined with a description of the thermodynamics of the upper soil levels (e.g., Giorgi et al. 2001) plus, possibly, other components of the earth system (e.g., marginal seas, lakes). They are forced by time-variable conditions along the lateral atmospheric boundary, sometimes also with large-scale constraints in the interior. These constraints are taken from either global model scenarios (e.g., Christensen and Christensen 2003) or from global reanalyses (e.g., Feser et al. 2001). Simulation lengths are several decades of years.

The purpose of regional climate modeling is to provide additional detail beyond the resolution of global reanalyses or global climate simulations. The enhanced spatial resolution of a RCM is thought to allow for a better description of the atmospheric dynamical processes, which lead to the formation of mesoscale features [such as fronts or mesoscale disturbances (e.g., Denis et al. 2002)]. The dependency of the smaller scales on the larger scales is considered to be better described ["downscaling" (von Storch 1995)]. Another benefit is that the influences of the physiographic detail, such as surface vegetation characteristics, coastlines, or complex topography, are better captured (e.g., Jacob and Podzun 1997). Thus, the theater of regional weather is considered to be made up from two main influences, namely, the large-scale atmospheric state and the regional physiographic detail.

The global analysis or simulation is assumed to reliably describe the dynamics of the large scales. The RCM should be better than the global analysis or simulation on medium spatial scales (600 km and less). Thus, the expected added value of regional climate modeling is mainly on these medium scales (e.g., Laprise 2003).

The concept of scale separation is used to analyze limited area model (LAM) results on different scales. It can serve as a tool for model evaluation or to explain the connection between weather phenomena with varying size. The concept was also incorporated into the spectral nudging or large-scale forcing concept by Waldron et al. (1996) and von Storch et al. (2000), which keeps the large-scale part of a regional model solution close to the forcing global field in the model interior. In the past, LAM fields were mainly looked

Corresponding author address: Dr. Frauke Feser, Institute for Coastal Research, GKSS Research Centre, Max-Planck-Str. 1, 21502 Geesthacht, Germany.
E-mail: feser@gkss.de

upon as a whole not separated into different spatial scales to study processes, to predict the regional climate, or to resolve regional weather details at a high resolution. Whenever filters were applied, this was generally done to filter in time. In this work the use of a spatial filter is proposed in order to separate the LAM results into several independent spatial-scale bands. The individual fraction of the regional model in adding value to the global model solution can thus be estimated. An explicit comparison with the forcing global model and observational reference data can assess the regional model simulation quality.

2. Models used for comparisons

In the following, the hypothesis that the regional models describe the phenomena on both large- and medium-scale bands better than the driving large-scale state will be tested. To do so, the case of an extended simulation is considered with the regional climate model REMO (Jacob and Podzun 1997) forced with global 6-hourly National Centers for Environmental Prediction–National Center for Atmospheric Research (NCEP–NCAR) reanalyses (hereafter referred to as the NCEP reanalyses) (Kalnay et al. 1996) from 1958 to 2002, which are given on a horizontal grid of about 2°.

REMO is a gridpoint model featuring the discretized primitive equations in a terrain-following hybrid coordinate system. The prognostic variables are surface air pressure, temperature, horizontal wind components, specific humidity, and cloud water. The physics scheme applied is a version of the global model ECHAM4 physics of the Max Planck Institute for Meteorology adapted for the regional model. The integration area has a horizontal spherical grid spacing of 0.5° (~47–55 km in zonal direction, ~55 km in meridional direction) and 81 × 91 grid points. The region considered is western Europe, extending about 4300 km longitudinally and 5000 km latitudinally. In the vertical 20 hybrid model levels are adapted to the orography close to the surface. The time step of the calculation is 5 min. A more detailed description of the multidecadal simulation is given in Feser et al. (2001).

The LAM was forced with 6-hourly NCEP reanalyses over the whole integration period from 1958 to 2002. The horizontal grid size of the reanalyses is about 1.875° longitudinally and latitudinally (T62 Gaussian grid). Because of the rotated spherical grid used by the LAM, its coverage with NCEP grid boxes is inhomogeneous with maximum resolution improvement in the southern part of the integration area. One LAM simulation was done in the conventional setup with lateral and surface forcing only, another one with additional "nudging of large scales" (von Storch et al. 2000). Nudging of large scales keeps the simulated state close to the driving state at larger scales, while allowing the model to freely generate medium-scale features consistent with the large-scale state. This is achieved by adding nudging terms in the spectral domain for the horizontal wind components above 850 hPa with maximum strengths for low wavenumbers at the top model level.

The LAM results were compared with the NCEP reanalyses at different spatial scales. To transfer the coarse-grid reanalyses to the 50-km grid used by the RCM, the reanalysis atmospheric fields were horizontally interpolated according to a 16-point formula as explained in Doms et al. (1995). The sea level pressure (SLP) is computed following Doms et al. (1995) by first calculating an extrapolation of the temperature T^* at the height of the LAM orography using the temperature T_{KE} of the lowest model level,

$$T^* = T_{\mathrm{KE}} + 0.0065\frac{R}{g}T_{\mathrm{KE}}\left(\frac{p_s}{p_{\mathrm{KE}}} - 1\right), \tag{1}$$

whereby p_s is the unreduced surface pressure and p_{KE} is the pressure at the lowest model level.

Then, the temperature T_{SL} at sea level and the mean temperature gradient γ are computed:

$$T_{\mathrm{SL}} = T^* + \gamma\frac{\Phi_s}{R}, \tag{2}$$

with the orography $\Phi_s = g \times z_s$ and $\gamma = 0.0065R/g$.

The orography used was taken from the LAM to account for better comparability of the results.

SLP is then computed as

$$p_{\mathrm{SL}} = p_s \exp\left\{\frac{\Phi_s}{RT^*}\left[1 - 0.5\frac{\gamma\Phi_s}{RT^*} + 0.333\left(\frac{\gamma\Phi_s}{RT^*}\right)^2\right]\right\}. \tag{3}$$

Accordingly, the 2-m temperature was calculated using the horizontally interpolated reanalyses temperature fields.

Reference dataset analyses of Germany's National Meteorological Service (DWD) are used. They were calculated with the "Europe Model" of the DWD on a rotated spherical grid with hybrid model levels and were available every 6 h. The same rotated North Pole and model grid was used as in the LAM simulation so that a straightforward comparison was possible.

3. Filter application

To analyze the above-described simulation data an isotropic digital filter was used (Feser and von Storch 2005). It is able to separate the LAM's model results into different spatial scales by filtering certain wavenumber ranges. The digital two-dimensional filter uses

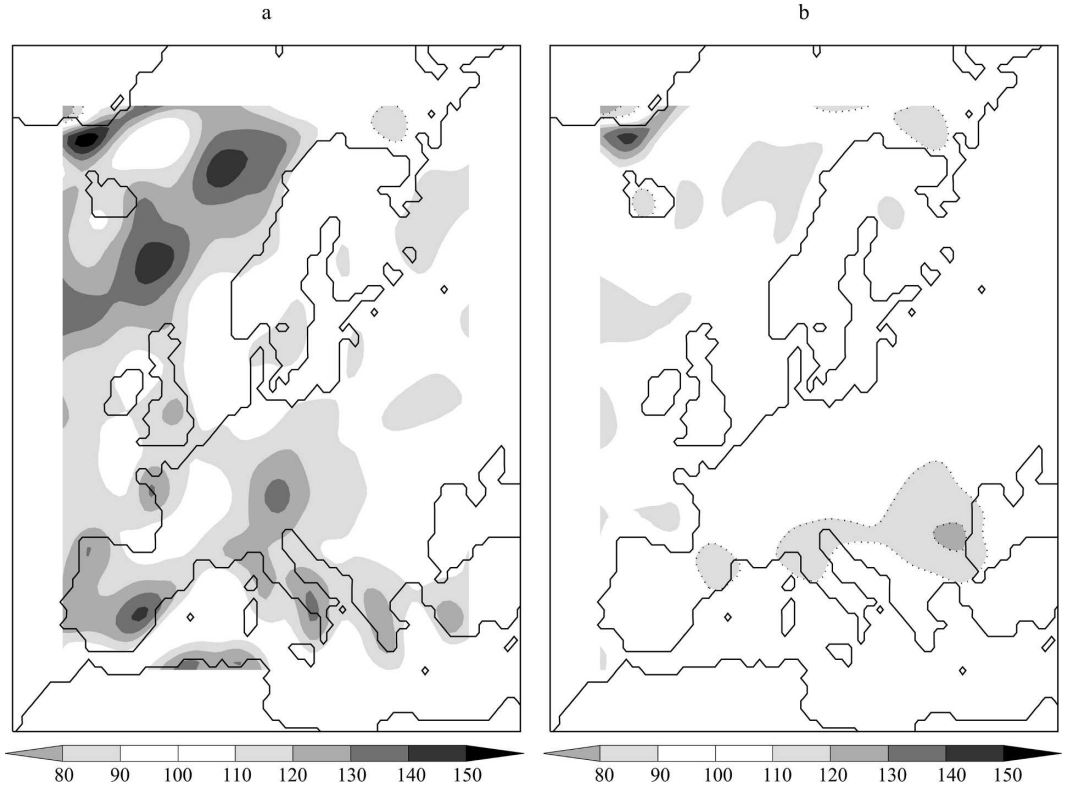

FIG. 1. Ratio of standard deviations, in percent, of low-pass-filtered 2-m temperature for JJA 1992–99: (a) DWD analyses/NCEP reanalyses and (b) DWD analyses/LAM simulation. Values of 90% and below are also drawn as dotted contour lines.

a footprint of 17 × 17 grid points to determine large-scale, medium-scale, and small-scale features from a field of 81 × 91 grid points. The filter weights are determined so that the 2D response function is approximately isotropic and for predetermined wavenumber ranges close to one or close to zero. In this context only the low-pass and the medium-pass filters are used.

The filter parameters were chosen as explained in Feser and von Storch (2005; see their Fig. 4 of the filter response function). For the low-pass filter a wavenumber range of 0–6 was chosen, which means that weather phenomena larger than about 700 km can pass this filter. The medium-pass filter was set to only let pass wavenumbers 8–16, which correspond to scales of about 550–250 km. These wavenumber ranges were selected to describe the scales that should be best resolved in the global model (low-pass filter) and the scales that are assumed to be best resolved in the LAM (medium-pass filter).

4. Temperature and sea level pressure comparisons

Both the RCM simulations and NCEP reanalyses are compared to operational high-resolution regional analyses, which have been constructed for routine regional weather forecasts by the DWD. The DWD analyses are considered as a "true" reference. It is expected that the RCM compares to the reference about as well as the driving NCEP reanalyses for large scales; on the medium scales, however, a significantly improved performance of the RCM is assumed.

Two variables are considered, namely, the spatially smooth air pressure and the spatially heterogeneous air temperature at or near the surface. The DWD temperature data are available from 1992 to 1999, for SLP only in 1994, 1995, 1998, and 1999. The data of the LAM, the NCEP reanalyses, and the DWD analyses were filtered and compared at the two spatial-scale ranges described before.

The percentage ratio of standard deviations of low-pass-filtered 2-m temperature DWD analyses to NCEP reanalyses for summers 1992 to 1999 is shown in Fig. 1a and the percentage ratio of standard deviations of low-pass-filtered 2-m temperature DWD analyses to the regional model run using spectral nudging for the same period in Fig. 1b. The ratio between the analyses and NCEP is mostly above 100%, indicating higher near-surface temperature variability in the DWD analyses,

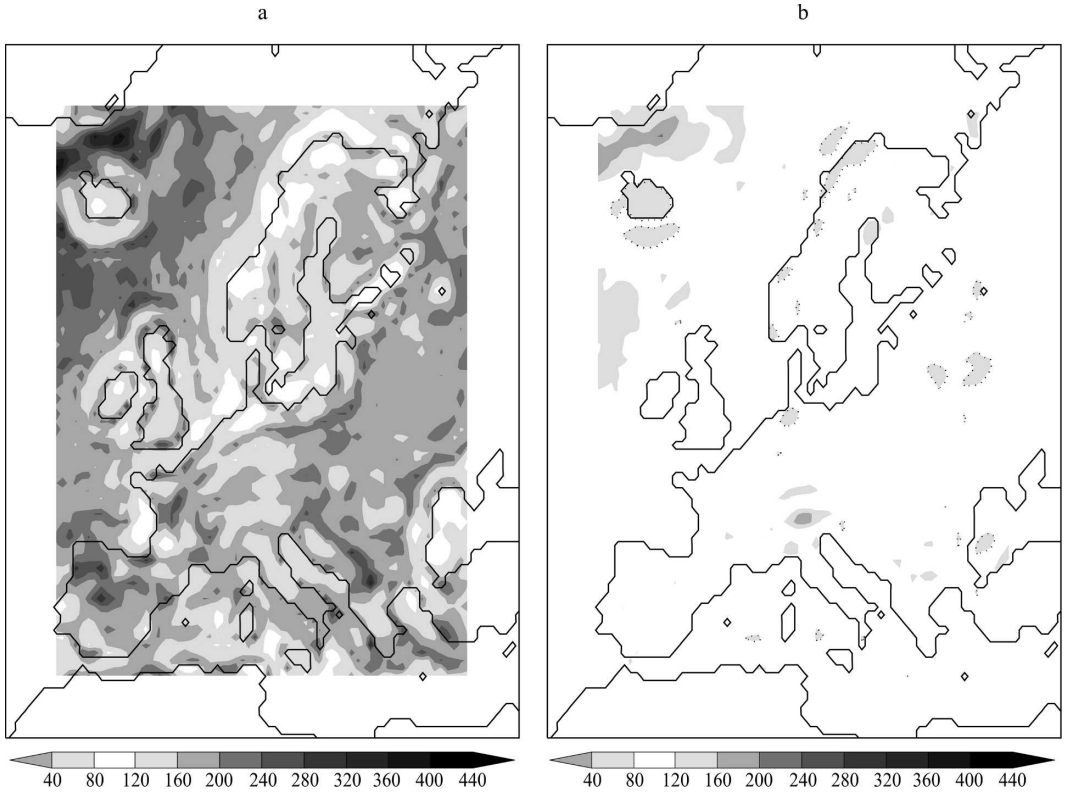

FIG. 2. As in Fig. 1 but for the medium-pass-filtered temperature. Values of 80% and below are also drawn as dotted contour lines.

especially over the North Atlantic with a factor of up to 1.5. The ratio between DWD and LAM shows smaller values: they range from 80% to 120% apart from a small area at the southeastern tip of Greenland. Even though a slightly higher agreement can be seen between the low-pass-filtered LAM and the reference data than between NCEP and the reference data, this is not the scale that should be the best resolved one of the LAM, the one where most added value could be assumed. The regional model results should be interpreted with caution at this scale; the higher ratio does not necessarily imply added value. Therefore the following figures will focus on medium-scale-filtered data.

Figure 2 shows the ratio of standard deviations of medium-pass-filtered 2-m temperature DWD analyses (a) to NCEP reanalyses and (b) to the regional model run using spectral nudging, in percent, for summers 1992 to 1999. Obviously the more highly resolved analyses show a much higher variability in the near-surface temperature than NCEP, up to a factor of 4.4. All values are above 100%, and hence the variability of the DWD analyses is higher at every grid point than the NCEP variability. The comparison of the LAM and the DWD results shows high agreement. The variability in the near-surface temperature is about the same in both simulations with only few areas of slight discrepancies. Figure 3 shows the same as Fig. 2 but now for winter. A similar pattern can be seen, with high variability for the analyses and much smaller values for the coarser NCEP reanalyses. The variability is up to a factor of 3 higher in the analyses than in the reanalyses. Again, the LAM simulation is much closer to the reference dataset than the global forcing data.

Figure 4 shows the ratio, in percent, of standard deviations of medium-pass-filtered SLP DWD analyses (a) to NCEP reanalyses and (b) to the LAM simulation using spectral nudging for winter 1998/99. The low-pass-filtered field was subtracted from the data prior to applying the medium-pass filter as explained in Feser and von Storch (2005) for achieving a better scale separation. An irregular pattern can be seen with many values above 100%. Large regions, especially in southern Europe, have larger SLP variability in the NCEP reanalyses than in the reference data whereby adjacent regions show the opposite combination. The reason for this effect is unknown. The comparison of DWD analyses and the LAM run shows mostly values around 100%. The ratio for the summer months (not shown)

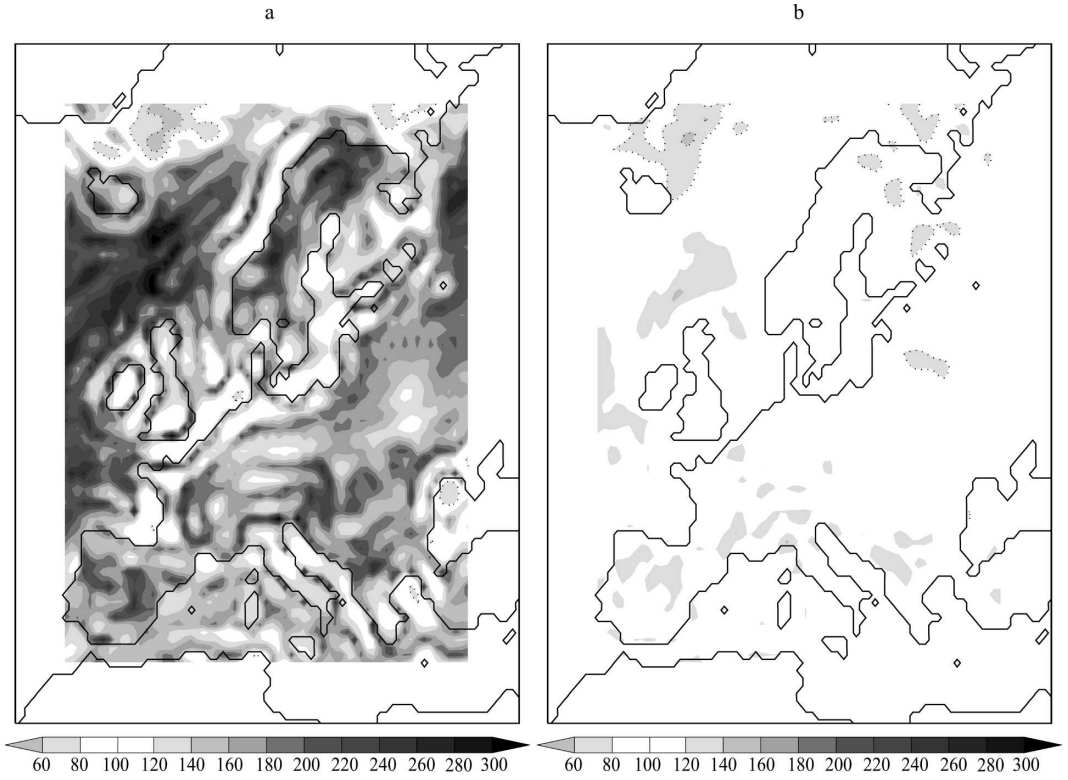

FIG. 3. As in Fig. 2 but for DJF 1992–99.

depicts the same sort of pattern, but the values are slightly larger.

5. Regional details

The modeled fields—unfiltered, low-pass- or medium-pass-filtered—are compared with the DWD reference with the "pattern correlation coefficient" ("pcc"; it is to be interpreted as a conventional correlation coefficient but this time across space) $P_{\mathrm{DWD}}(x)$ with x = NCEP, sn, and nn. "NCEP" represents the NCEP reanalyses, "sn" the RCM simulation with nudging of large scales, and "nn" the same without nudging of large scales. The results shown so far all dealt with "sn." The RCM simulation x is considered to be an improvement over NCEP if $\Delta_{x,\mathrm{NCEP}} = P_{\mathrm{DWD}}(x) - P_{\mathrm{DWD}}(\mathrm{NCEP}) > 0$. The pattern correlation coefficient of two spatial fields a and b with grid values a_i and b_i is formally the same as the sample correlation coefficient of a pair of time series:

$$P_a(b) = \frac{\sum_i (a_i - \bar{a})(b_i - \bar{b})}{\sqrt{\left[\sum_i (a_i - \bar{a})^2 \cdot \sum_i (b_i - \bar{b})^2\right]}}. \qquad (4)$$

Here $\bar{a}$ and $\bar{b}$ are the spatial means of a and b. The denominator features the spatial standard deviations of a and b.

In this article, the reference a is given by the DWD analyses, while the role of the second field b is taken over by the NCEP reanalyses, and the RCM simulations with (sn) and without (nn) nudging of large scales. Unfiltered fields and filtered fields are compared with each other.

Figure 5 shows time series of pcc for two sample seasons. The dependency of the RCM results on the large-scale forcing is apparent in the pressure pcc; large differences between NCEP and the DWD analyses coincide with even greater differences between the RCM simulations and the DWD analyses for the unfiltered and the low-pass-filtered fields. This effect is reduced by applying the nudging technique.

For the spatially smooth *pressure fields* the added value of the RCM simulations is limited to the medium scales and to the simulation with nudging of large scales. For *air temperature* anomalies, the pcc of the medium-pass-filtered and unfiltered fields are for the RCM simulations always higher than for the global reanalyses. Because of high fluctuation in pcc, especially for the NCEP reanalyses, a running average with a

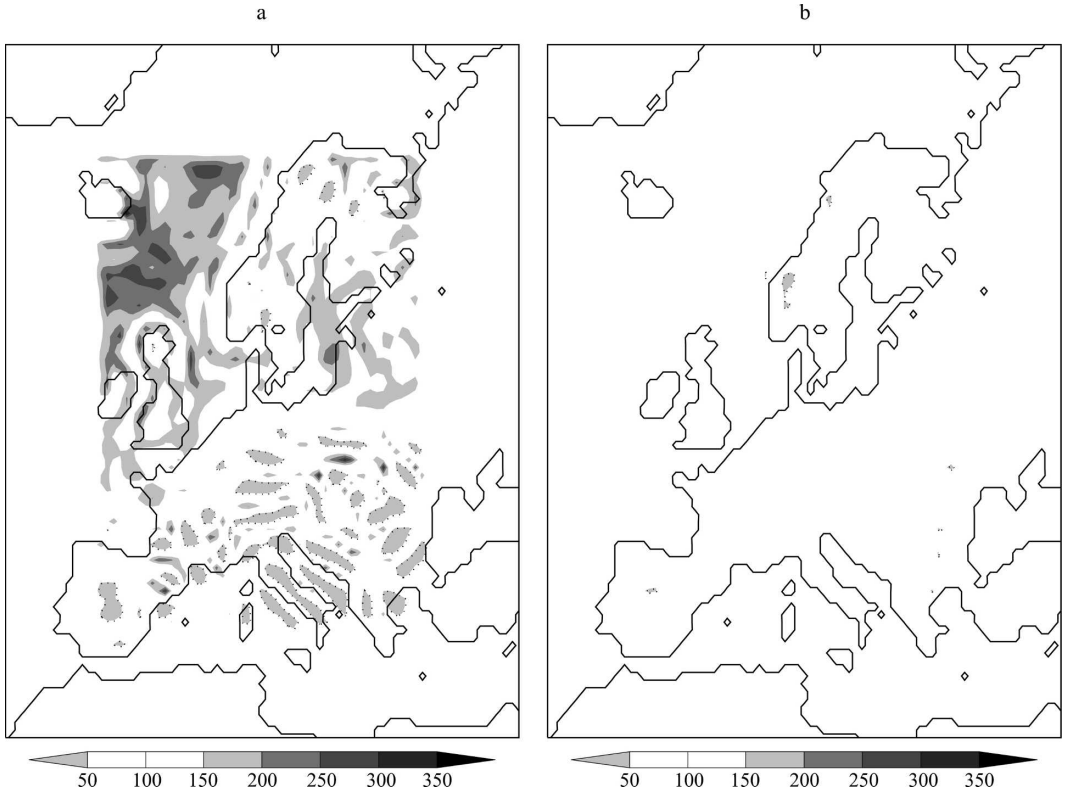

FIG. 4. As in Fig. 1 but of medium-pass-filtered SLP for DJF 1998/99. Values of 50% and below are also drawn as dotted contour lines.

length of 4 was applied for better readability of the figure. The largest added values are apparent again for the medium scales where the regional models were expected to give the best results. For the pcc of the low-pass-filtered fields the conventional RCM simulation shows a deterioration compared to the NCEP reanalyses. By contrast, when applying nudging of large scales a small added value is achieved (note that the nudging is toward the NCEP reanalyses, not toward the DWD analyses).

These findings are substantiated by Table 1, which is listing the mean pcc P_{DWD}(NCEP) for full and anomaly fields (i.e., deviations from the time-mean fields). Also, the differences $\Delta_{\mathrm{sn,NCEP}}$ and $\Delta_{\mathrm{nn,NCEP}}$ are listed. Positive differences are given in bold; statistically significant differences are marked with an asterisk.

The mean improvement in SLP for the regional model is 1.4% for winter and 4.1% for summer in case of nudging of large scales. No added value is provided for the standard RCM simulation. A similar result is obtained for the SLP anomalies, that is, for deviations from the long-term mean.

The result is much more encouraging for air temperature. Simulations with nudging of large scales return significant added value in both seasons for all spatial scales. When anomalies are considered, large-scale pcc increases by 5.5% and 6.3% in December–January (DJF) and June–August (JJA), and the medium-scale pcc by 21.5% and even 30.4%. Without nudging of large scales, no added value is obtained for large scales, but there is a significant increase in terms of medium-scale pcc.

It is emphasized that this analysis describes only one measure of added value. There may be other useful measures, and it may be that also in case of the conventional setup a more pronounced added value emerges from such a measure.

Case studies for selected weather situations

To get an idea of the different patterns that are associated with high and low pcc values some examples were calculated for near-surface temperature and SLP. Figure 6 shows an example of high similarity between the LAM results and the DWD analyses. Shown are anomalies of medium-pass-filtered 2-m temperature fields for 0600 UTC 30 August 1998. The upper left panel shows the DWD reference data, the upper right panel the NCEP reanalyses, the lower left panel the

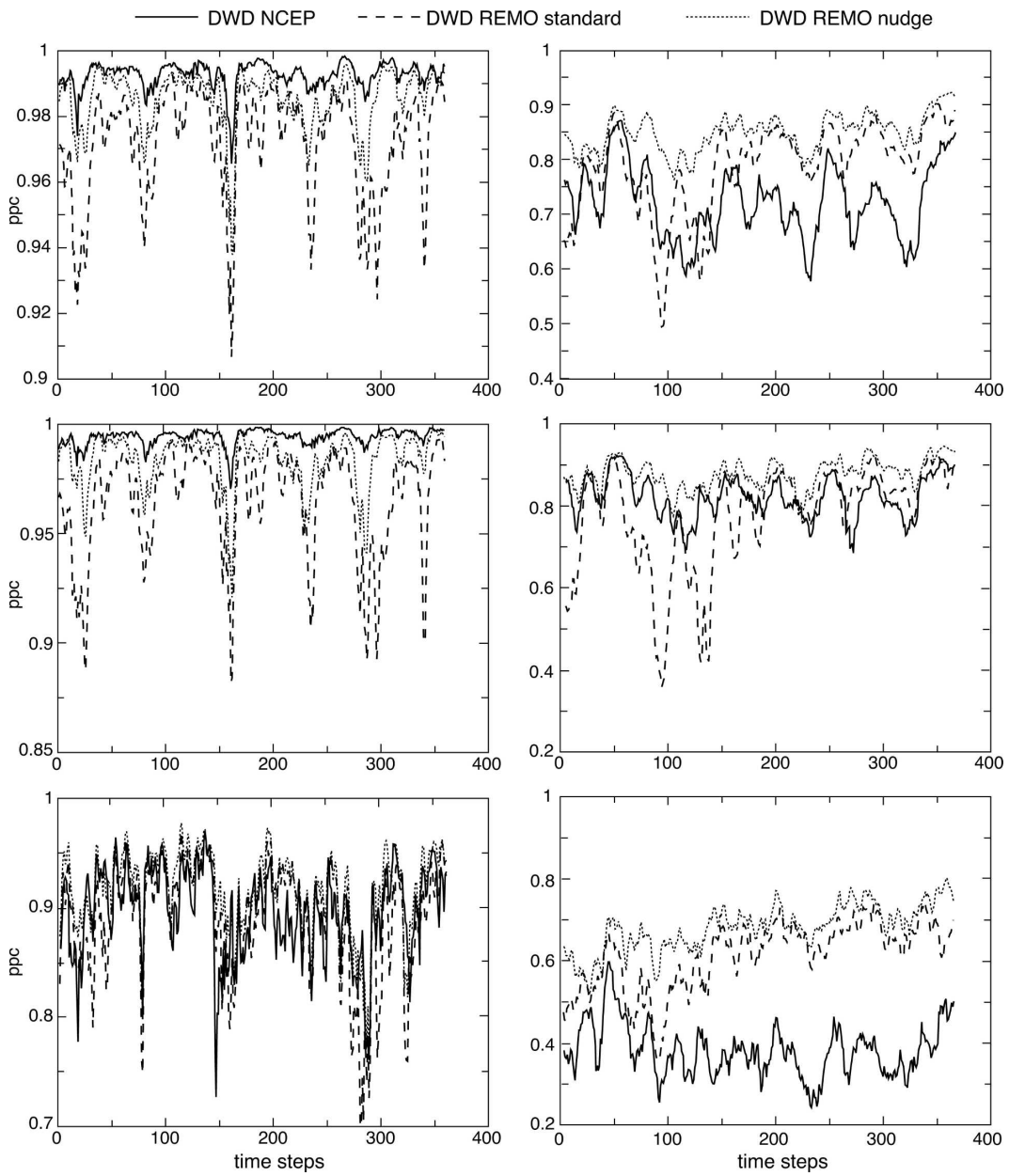

FIG. 5. (left) Six-hourly time series of SLP pattern correlation coefficients for winter 1998/99; (right) time series of 2-m temperature anomaly pcc for summer 1998: (top) for full fields and for (middle) low-pass- and (bottom) medium-pass-filtered fields.

LAM results with nudging of large scales, and the lower right panel the LAM temperatures for the conventional run. Also plotted are dotted contour lines of unfiltered SLP. This example is a case of better performance of the LAMs than NCEP. The medium-scale temperature anomaly pcc are 88.1% for the LAM with nudging of large scales and 80.9% without nudging. NCEP has a pcc of 9.6% for this date and shows deviations in the temperature pattern for the Mediterranean area as well as for Scandinavia, England, and Ireland in comparison with the analyses. The LAM results are closer to the DWD temperature pattern for these regions. The pressure fields do not show large deviations between the different simulations.

Figure 7 is an example for higher SLP pcc values for the NCEP reanalyses than for the LAM results. Again, anomalies of medium-pass-filtered 2-m temperature are plotted, this time for 1800 UTC 22 June 1998. The

TABLE 1. (middle column) Time-mean pattern correlation coefficients P_{DWD}(NCEP) (%) of pairs of DWD and NCEP analyzed regional fields, and (two right columns) mean differences when NCEP is replaced by REMO simulation with ($\Delta_{sn,NCEP}$) and without ($\Delta_{nn,NCEP}$) nudging of large scales. Positive numbers, given in bold, indicate an improvement over the NCEP reanalyses; negative values a deterioration; 95% significant deviations are marked by an asterisk.

Variable	Season	Field	P_{DWD}(NCEP)	$\Delta_{sn,NCEP}$	$\Delta_{nn,NCEP}$
		Full fields			
SLP	DJF	Unfiltered	99.4	−0.7*	−2.2*
		Low pass	99.6	−1.0*	−3.4*
		Medium pass	91.3	**1.4***	−1.1*
SLP	JJA	Unfiltered	98.0	−2.0*	−8.0*
		Low pass	98.5	−2.6*	−11.6*
		Medium pass	84.2	**4.1***	−0.6
T	DJF	Unfiltered	96.0	**1.0***	**0.5***
		Low pass	95.8	**0.8***	−0.8*
		Medium pass	76.9	**3.6***	**1.5***
T	JJA	Unfiltered	95.8	**1.4***	**0.5***
		Low pass	96.3	**0.8***	−1.0*
		Medium pass	65.4	**10.4***	**6.1***
		Anomaly fields			
SLP	DJF	Unfiltered	99.1	−0.9*	−2.9*
		Low pass	99.3	−1.3*	−4.2*
		Medium pass	89.6	**1.0***	−2.0*
SLP	JJA	Unfiltered	98.3	−1.9*	−8.9*
		Low pass	98.6	−2.7*	−12.9*
		Medium pass	84.9	**2.6***	−3.0*
T	DJF	Unfiltered	70.7	**9.8***	**6.2***
		Low pass	79.2	**5.5***	−0.5*
		Medium pass	27.0	**21.5***	**15.5***
T	JJA	Unfiltered	70.2	**13.2***	**7.8***
		Low pass	80.2	**6.3***	−2.5*
		Medium pass	36.0	**30.4***	**24.3***

pressure field of the reanalyses is closer to the DWD data than the regional simulations. The LAM results show deviations compared to the operational analyses, especially the one without nudging of large scales. The pcc values for the unfiltered SLP fields are 98.2% for the NCEP reanalyses, 97.2% for the LAM with, and 60.7% for the LAM without nudging of large scales. For the LAM simulation without nudging of large scales the influence of the pressure field on the temperature pattern can be seen for Sweden and the northern Baltic Sea area as well as for the eastern boundary of the integration domain. A high pressure system of 1030 hPa was simulated by the regional model that was nonexistent in the operational analyses. The medium-scale temperature anomalies pattern, hence, looks quite different from the DWD data in this area. For the southern part of the integration domain both LAM simulations are much closer to the operational analyses than NCEP. The medium-scale temperature anomaly pcc is 29.2% for the NCEP reanalyses, 57.7% for the LAM with, and 36.8% for the LAM without nudging of large scales. Even though the SLP pattern was best described by the reanalyses, the high-resolution temperature field was not well interpreted by them. It is reasoned that these are dynamically induced regional temperature details that could not be resolved by the coarse-resolution global reanalyses and that additional information could be added by the RCMs on the spatial scale that was considered.

6. Summary and conclusions

An isotropic digital spatial filter was applied to evaluate and analyze LAM results separately at different spatial scales. The idea is that regional models mainly add detail at the specific scale for which they were constructed; this means that for detection of an added value a scale separation of the model results is reasonable. Ratios of standard deviations of filtered near-surface temperature and SLP fields between regional model simulations or global reanalyses and an operational analysis were calculated. Hereby, the LAM showed larger variability than the global reanalyses and its values were comparable to those of the reference dataset. The result was more distinct for the more regional quantity near-surface temperature than for the larger-scale SLP. As a means for the skill of the individual simulations, pattern correlation coefficients were computed between the models and the reference analyses. For SLP, an added value can be found for the regional model simulation in the case of nudging of large scales for the medium-pass-filtered results. For the standard RCM simulation this is not possible with the presented method. Since SLP is a rather large-scale quantity the focus is put on near-surface temperature in order to detect an added value on the medium scales. The pattern correlation coefficients between the regional model results and the reference data are higher than the global reanalyses pattern correlation coefficients for the unfiltered and the medium-pass-filtered temperature fields. With nudging of large scales an improvement also for the large scales could be achieved. Consistent with the concept of downscaling, an improvement in the representation of large scales is associated with an improvement of the simulation at the medium scales. When the role of the physiographic detail is less important, as in the case of *air pressure*, the overall added value is small; in that case, the RCM has hardly a chance to improve the large-scale field, as the only relevant factor available is the driving reanalyses. The situation is different in terms of *air temperature* because the regional dynamics of this variable depends

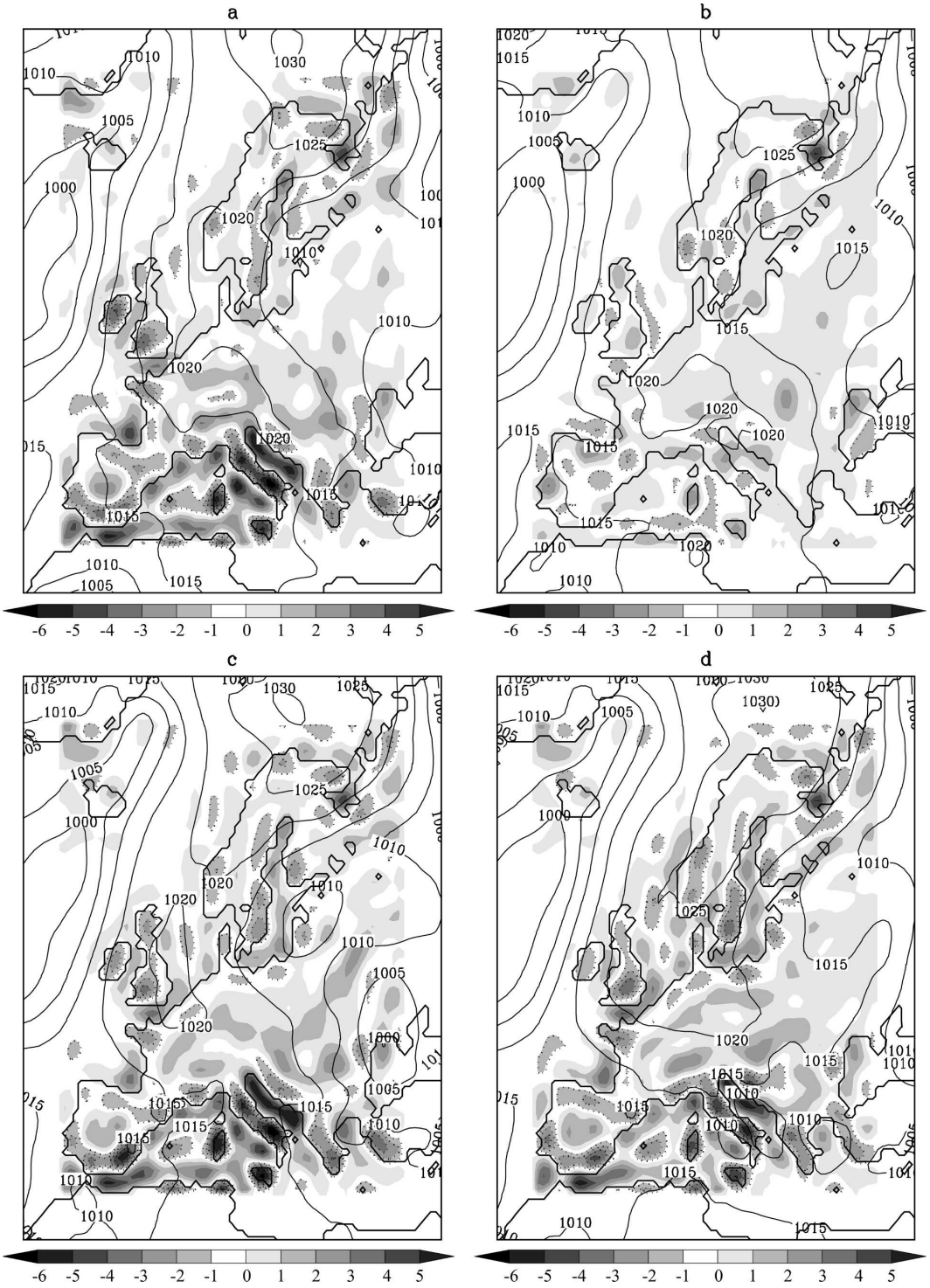

FIG. 6. Anomalies of medium-pass-filtered 2-m temperature (K) fields (shaded) and unfiltered SLP isobars (hPa): (a) DWD, (b) NCEP, (c) LAM_{sn}, and (d) LAM_{nn} for 0600 UTC 30 Aug 1998. Negative temperature anomalies are also drawn as dotted contour lines to enable differentiation from positive values.

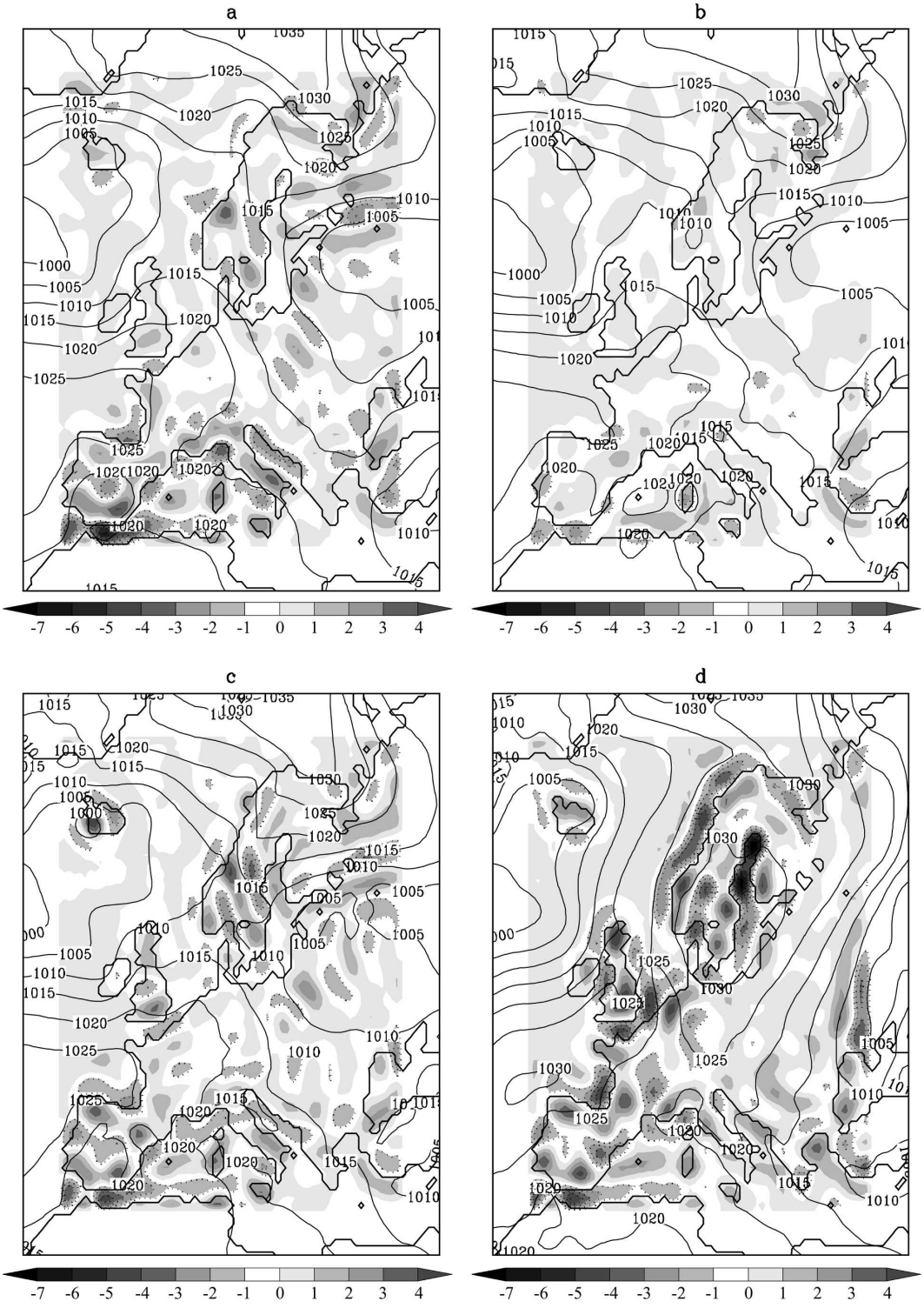

FIG. 7. As in Fig. 6 but for 1800 UTC 22 Jun 1998.

strongly on the physiographic detail. Therefore, the RCM is capable of improving the simulation not only of the medium-scale temperature fields but also of the large-scale field. By comparing the results for full fields and for anomaly fields, it is found that the added value is not mainly related to an improvement of time-mean fields but is apparent in the anomalies as well. A maximum improvement is given for temperature anomalies

at the medium scales; the regional model run with nudging of large scales gives a pattern correlation coefficient that is on average more than 30% higher than the pattern correlation coefficient of the global reanalyses. The results show that the main achievements of a RCM can be seen at smaller spatial scales while only little added value is given at the larger scales, which are already well resolved in the global forcing model. Therefore it is proposed to use spatial filters to look at the regional model results separated into different spatial scales in order to detect additional information given by the high-resolution model. The analysis of RCM results separated into different spatial domains presented in this work revealed significant added value on the regional scale.

Acknowledgments. The author thanks R. Laprise and H. von Storch for valuable discussions regarding this work. B. Gardeike prepared some of the figures for this paper. The author also thanks the German Climate Computing Center (DKRZ), which provided the computer hardware for the multidecadal LAM simulation in the project "Anthropogenic and natural regional environmental change." The NCEP reanalyses data were provided by the National Center for Atmospheric Research. The author also thanks Germany's National Meteorological Service for providing the operational analyses.

REFERENCES

Butler, D., 2003: Heatwave underlines climate-model failures. *Nature,* **424,** doi:10.1038/424867a.

Christensen, J., and O. Christensen, 2003: Severe summertime flooding in Europe. *Nature,* **421,** 805–806.

Denis, B., R. Laprise, D. Caya, and J. Côté, 2002: Downscaling ability of one-way nested regional climate models: The Big Brother Experiment. *Climate Dyn.,* **18,** 627–646.

Doms, G., and Coauthors, 1995: Dokumentation des EM/DM-Systems. Deutscher Wetterdienst Abteilung Forschung, Offenbach a.M., 550 pp. [Available from Deutscher Wetterdienst, Zentralamt, Abteilung Forschung, Postfach 10 04 65, 63004 Offenbach am Main, Germany.]

Feser, F., and H. von Storch, 2005: A spatial two-dimensional discrete filter for limited-area-model evaluation purposes. *Mon. Wea. Rev.,* **133,** 1774–1786.

——, R. Weisse, and H. von Storch, 2001: Multi-decadal atmospheric modeling for Europe yields multi-purpose data. *Eos, Trans. Amer. Geophys. Union,* **82,** 305–310.

Giorgi, F., and Coauthors, 2001: Regional climate information—Evaluation and projections. *Climate Change 2001: The Scientific Basis,* J. T. Houghton et al., Eds., Cambridge University Press, 583–638.

Jacob, D., and R. Podzun, 1997: Sensitivity studies with the Regional Climate Model REMO. *Meteor. Atmos. Phys.,* **63,** 119–129.

Kalnay, E., and Coauthors, 1996: The NCEP/NCAR 40-Yr Reanalysis Project. *Bull. Amer. Meteor. Soc.,* **77,** 437–471.

Laprise, R., 2003: Resolved scales and nonlinear interactions in limited-area models. *J. Atmos. Sci.,* **60,** 768–779.

von Storch, H., 1995: Inconsistencies at the interface of climate impact studies and global climate research. *Meteor. Z.,* **4,** 72–80.

——, H. Langenberg, and F. Feser, 2000: A spectral nudging technique for dynamical downscaling purposes. *Mon. Wea. Rev.,* **128,** 3664–3673.

Waldron, K. M., J. Paegle, and J. D. Horel, 1996: Sensitivity of a spectrally filtered and nudged limited-area model to outer model options. *Mon. Wea. Rev.,* **124,** 529–547.